First-Principle Study on Lead-Free Perovskite for Optoelectrical Applications

H. Abdulsalam [1]* and G. Babaji [2]

[1]Department of Physics, Yobe State University, Damaturu P.M.B.1144, Yobe Nigeria
[2]Department of Physics, Bayero University, Kano P.M.B. 3011, Kano Nigeria
**Corresponding author E-mail*: ahassanabdulsalam@gmail.com
(Received 13 March 2023, Accepted 15 June 2023, Published 26 June 2023)

Abstract

The research into new types of light harvesters for solar cells is driven by the need to increase their efficiency and make them more reliable. One promising material for replacing the dye-molecule light harvesters is the Organometallic perovskite; the most popular among them is methyl ammonium lead iodide, $CH_3NH_3PbI_3$. Although methyl ammonium lead iodide, ($CH_3NH_3PbI_3$) has proven to be an effective photovoltaic material, there remains a huge concern about the toxicity of lead. An investigation into the possible replacement of lead (Pb) with Germanium (Ge), Silicon (Si), and Tin (Sn) in $CH_3NH_3PbI_3$ was carried out. Before this investigation, structure building, parameter optimization, determination of the best exchange functional, k-grid convergence test, and determination of equilibrium lattice constant and geometry relaxation were carried out for the first set of materials. Visualization for Electronic and Structural Analysis (VESTA) and Avogadro software were used for the structure building while FHI-aims code was used to simulate these Perovskites materials. The BLYP (a parameterization of GGA) exchange functional gave the minimum single-point energy at a minimum run time for all the structures. The lattice constants obtained using Phonopy (with zero-point energy) are 5.894, 5.907, 6.248, 5.950, and 6.049 Å for $CH_3NH_3GeBr_3$, $CH_3NH_3GeI_3$, $CH_3NH_3PbI_3$, $CH_3NH_3SiI_3$ and $CH_3NH_3SnI_3$ respectively. The energy band gap calculated for the second set of materials: $CH_3NH_3GeI_3$, $CH_3NH_3PbI_3$, $CH_3NH_3SiI_3$, $CH_3NH_3SnI_3$, and $CH_3NH_3GeBr_3$ at their respective equilibrium lattice constants are 1.606, 1.513, 1.804, 1.051 and 1.925 eV respectively. These calculated band gap values were compared with reported theoretical and experimental values. There is a close agreement in calculated lattice constants and bandgaps with reported theoretical and experimental values. Dielectric constants, refractive index extinction coefficient, absorption coefficient, reflectivity, and optical conductivity of these materials were also determined. The optical properties obtained show that Sn and Ge are a good choice for the replacement of Pb; also, the optical properties obtained indicate that these materials have other possible applications in areas other than photovoltaic technology.

***Keywords*:** Organometallic-perovskite; DFT, FHI-aims; Energy-bandgap; lattice-constant; dielectric constants; refractive-index; extinction-coefficient; absorption; coefficient; reflectivity; optical conductivity

1. INTRODUCTION

To design an efficient solar cell device, a deep understanding of underlying material's properties such as mechanical, electrical, and optical properties are required. Quantum mechanical approaches provide a deep understanding of properties of many body systems such as mechanical, electrical, and optical properties. Among the available theoretical approaches, the density-functional theory (DFT) has become overwhelmingly popular. Its success greatly relies on the existence of efficient computer numerical codes. In these numerical codes the input parameters can be adjusted. The overall principles of DFT are based on the Hohenberg–Kohn's theorems [1]. DFT has a strong versatility especially in the description of the ground state properties of semiconductors and metals. Increase in computing power has afforded further capabilities in system's size that DFT methods can handle.

In the last few years, the advent of metal halide perovskite solar cells has revolutionized the prospects of next-generation Photovoltaics cells. As this technology as develop in an exceptional rate, research into the environmental impact is becoming increasingly relevant. The drawback of metal halide perovskites in their current form is that they contain heavy metals[2]. Unfortunately, the most efficient perovskite solar cells all contain lead (Pb), which is an unsettling flaw that leads to severe environmental concerns and is therefore a stumbling block envisioning their large-scale application[3]. Regulation and common sense suggest that PSCs have to become lead free to deliver a sustainable technology[4]. Given the above facts, the realization of a lead-free halide perovskite that can compete with Lead-based halide perovskite is of outstanding interest.

This work tends to look into the possible replacement of $CH_3NH_3PbI_3$ with other lead-free organometallic perovskites as the active layer in perovskite solar cell. The choice of the best replacement will be determined by the values of the electronic and optical properties obtained from the material(s) resulting from replacement of lead. Band structure analysis and energy bandgap calculations were performed. Furthermore, dielectric constants, refractive index, the extinction coefficient, the absorption coefficient, the reflectivity and the optical conductivity of these materials were determined.

2. THEORETICAL BACKGROUND

2.1 DENSITY FUNCTIONAL THEORY

Density Functional Theory (DFT) is a quantum mechanical technique used in Physics and chemistry to investigate the structural and electronic properties of many body systems. DFT has proved to be highly successful in describing structural and electronic properties in a vast class of materials, ranging from atoms and molecules to simple crystals and complex extended systems (including gasses and liquids). For these reasons DFT has become a common tool in first-principles

calculations aimed at describing or even predicting properties of molecular and condensed matter systems [5]. Traditional methods in electronic structure theory, in particular Hartree-Fock theory and its descendants are based on the complicated many-electron wave function. The main objective of density functional theory is to replace the many-body electronic wave function with the electronic density as the basis quantity. Whereas the many-body wave function is dependent on 3N variables, three special variables for each of the N electrons, the density is only a function of three variables and is a simpler quantity to deal with both conceptually and practically.

2.2 Lattice constant

The lattice constant, or lattice parameter, refers to the physical dimension of unit cells in a crystal lattice. Lattices in three dimensions generally have three lattice constants, referred to as *a*, *b*, and *c*. However, in the special case of cubic crystal structures, all of the constants are equal referred to as *a*. Lattice parameter as a function of temperature and composition is an important piece of information for the modeling of structural changes in solids. Different regions in a solid microstructure impose mechanical constraint on each other, and thus when the lattice parameters change in any region due to temperature or composition variations or due to a structural phase transformation, local elastic strains and stresses will develop, which can profoundly affect the structure of the solid[6].

2.3 Electronic Band Structure

The periodic crystal structure is one of the most important aspects of materials science as many properties of materials depend on their crystal structures. One of its most immediate consequences is the arrangement of the electronic states within bands. For semiconductors, many properties are determined from these bands[7]. The electronic band structure of a solid describes those ranges of energy that an electron within the solid may have and ranges of energy that it may not have[8]. Band theory derives these bands and band gaps by examining the allowed quantum mechanical wave functions for an electron in a large periodic lattice of atoms or molecules. Band theory has been successfully used to explain many physical properties of solids, such as electrical resistivity and optical absorption, and forms the foundation of the understanding of all solid-state devices. Band structure calculations take advantage of the periodic nature of a crystal lattice, exploiting its symmetry.

The electronic band gaps of hybrid organic-inorganic Perovskite halide materials are determined by the Highest Occupied Molecular Orbital (HOMO) energy Level (which is similar to valence band maximum (VBM) in the inorganic semiconductor and Lowest Unoccupied Molecular Orbital (LUMO) energy level (which is also similar to conduction band minimum (CBM) in the inorganic semiconductor. A requisite for PSC to work properly, the LUMO level of the light harvester should be higher than the conduction band edge (CBE) of anode material[9]; for example in TiO_2 which is located at -4.0 eV [10]. This would provide the required driving force for a faster excited state electron injection. The magnitude of the band gap determines the onset of optical

absorption and is closely related to the maximum voltage achievable in a photovoltaic device[11]. The energy band gaps of organic-inorganic perovskite increase with increasing lattice parameter, contrary to most general semiconductors like Si and GaAs, this is due to the electronic structure of the Perovskite materials[12]. It was found experimentally that the band gap of $CH_3NH_3PbI_3$ increases with lattice parameter, as evidenced by Photoluminescence (PL) results[13].

2.4 Dielectric Constant

Relative permittivity also known as dielectric constant is denoted as $\epsilon_r(\omega)$and is defined as

$$\epsilon_r(\omega) = \frac{\epsilon(\omega)}{\epsilon_o} \quad (1)$$

where $\epsilon(\omega)$ is the complex frequency-dependent permittivity of the material, and ϵ_o is the vacuum permittivity[14]. The dielectric constant is obtained from the response of the material to an external electric field; it depends on the frequency of the applied electric field and is described by a tensor for anisotropic system. The dielectric tensor $\epsilon_r$consists of a real part which represents the storage and an imaginary part which represents the loss[15]. The dielectric constant also called relative permittivity is value of the real part of the complex dielectric function at frequency equals to zero[16] i.e. $Re[\epsilon_r(\omega = 0)]$. The amount of electric field attenuated in a substance compared to that from a vacuum is indicated by its dielectric constant. Dielectric constant determines the magnitude of the coulomb interaction between electron-hole pairs and charge carriers as well as any fixed ionic charges in the lattice; high dielectric constants are required for high efficiency solar cell. Dielectric constant for $CH_3NH_3PbI_3$ is in the range of 5–7[17].For materials that possess permanent dipoles, there is a significant variation of the dielectric constant with temperature. This is due to the effect of heat on orientational polarization. However, the dielectric constant will not increase continually as temperature is lowered. There are several discontinuities in the dielectric constant as temperature changes. Dielectric constant changes suddenly at phase boundaries, this is because the structure changes in a phase change, and therefore dielectric constant is strongly dependent on the structure (DoITPoMS, 2017).

2.5 Other Optical Properties

The frequency-dependent complex dielectric function $\varepsilon(\omega)$ is directly related to the energy band structure of solids [18]. From the dependent complex dielectric function (i.e. real and imaginary parts) the following optical properties; refractive index $n(\omega)$, the extinction coefficient $k(\omega)$, the absorption coefficient $\alpha(\omega)$, the reflectivity $R(\omega)$ and the optical conductivity $\sigma(\omega)$ can be obtained[19].

Absorption coefficient

The absorption coefficient determines how far into a material light of a particular wavelength can penetrate before it is absorbed. In a material with a low absorption coefficient, light is only poorly absorbed, and if the material is thin enough, it will appear transparent to that wavelength. The absorption coefficient depends on the material and also on the wavelength of light which is being absorbed [20].

Optical conductivity

The optical conductivity is a material property, which links the current density to the electric field for general frequencies. In this sense, this linear response function is a generalization of the electrical conductivity, which is usually considered in the static limit [21].

Extinction coefficient

Extinction coefficient is the measure of the rate of diminution of transmitted light via scattering and absorption for a medium in other words it is the measure of the damping of the electromagnetic wave as it passes into a medium [22].

Reflectivity

Reflectivity is an optical property of material, which describes how much light is reflected from the material in relation to an amount of light incident on the material. The reflection occurs always on the surface of the material, for the light-diffusing (translucent) materials also in the volume of the material [23].

Refractive index

Refractive index is the measure of bending of a light ray when passing from one medium to another. It can also be defined as the ratio of the velocity of a light ray in an empty space to the velocity of light in a substance [24]. In electromagnetic waves, the speed is dependent on the optical density of the medium. Optical density is the tendency of the atoms in a material to restore the absorbed electromagnetic energy. The more optically dense material is, the slower the speed of light.

3. METHODOLOGY

3.1 Structure Building and Optimization of Parameters

The initial atomic fractional coordinates of cubic Methyl ammonium lead bromide ($CH_3NH_3PbBr_3$) with lattice constant $a = 5.933$ Å was obtained from literature [25], this is given in Table 3.5. The initial atomic fractional coordinates were used to build the structure of $CH_3NH_3PbI_3$ (without hydrogen atoms) using Visualization for Electronic and Structural Analysis (*VESTA).*

Table 1 *Structural Parameters of Cubic CH3NH3PbBr3, a=5.933 Å (without hydrogen atoms)*

Atom	*x*	*y*	*z*
Pb	0.0000	0.0000	0.0000
Br	0.0000	0.0413	0.5000
N	0.4130	0.4170	0.5000
C	0.5780	0.5820	0.5000

The adding of the hydrogen atoms and the replacement of Br_3 with I_3 was done using Avogadro software; this software has the facility for adding hydrogen. After the addition of the

hydrogen atoms, the resulting geometry parameter was used to build the geometries of $CH_3NH_3PbI_3$, $CH_3NH_3SnI_3$, $CH_3NH_3SiI_3$, $CH_3NH_3GeI_3$ and $CH_3NH_3GeBr_3$. The resulting geometries were standardized to take care of the different atomic radius of the different species.

Then some parameters were optimized by making a number of guess (these are series of values for each of the parameters) for getting the minimum energy at a reasonable time for each parameter, and for each material. These parameters are *occupation type (Gaussian or Fermi), charge mix param, initial moment, and n max pulay.* The appropriate *exchange functional* was also determined.

3.2 Band Structure Analysis

The optimized parameters are used in the band structure analysis, but in order to calculate the band gap, the high symmetry points in the reciprocal space have to be input in to the FHI-aims control.in file (Franz and Sergey, 2013). The high symmetry points in the reciprocal space for a simple cubic are given in Table 2. Using the path shown in figure 1, these high symmetry points were tagged with the *output band* tag in the control.in file.

Table 2 *High Symmetry K-points of Cubic Lattice (Setyawan & Curtarolo, 2010).*

0.0	0.0	0.0	Γ
0.5	0.5	0.0	M
0.5	0.5	0.5	R
0.0	0.5	0.0	X

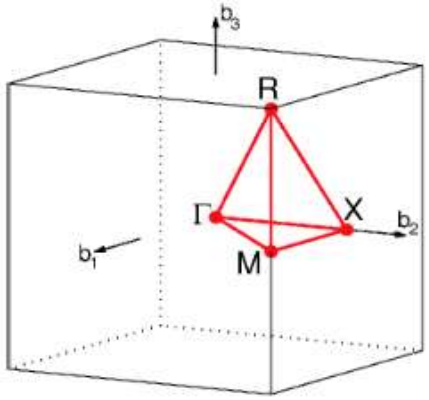

Figure 1 *Brillouin Zone of Simple Cubic lattice, Path: Γ-X-M-Γ-R-X/M-R(Setyawan & Curtarolo, 2010).*

3.3 Optical properties

From the complex dielectric function $\varepsilon(\omega)$, (i.e. real and imaginary parts) the following optical properties; refractive index $n(\omega)$, the extinction coefficient $k(\omega)$, the absorption coefficient $\alpha(\omega)$, the reflectivity $R(\omega)$ and the optical conductivity $\sigma(\omega)$ are obtained using the following formulae[26]:

Absorption coefficient:

$$\alpha(\omega) = \frac{\sqrt{2}\,\omega}{c}\sqrt{\left(\sqrt{\left(\varepsilon_1(\omega)\right)^2 + \left(\varepsilon_2(\omega)\right)^2}\right) - \varepsilon_1(\omega)} \qquad (2)$$

Refractive index:

$$n(\omega) = \sqrt{\frac{\sqrt{\left(\varepsilon_1(\omega)\right)^2+\left(\varepsilon_2(\omega)\right)^2}+\varepsilon_1(\omega)}{2}} \qquad (3)$$

Extinction coefficient:

$$k(\omega) = \sqrt{\frac{\sqrt{\left(\varepsilon_1(\omega)\right)^2+\left(\varepsilon_2(\omega)\right)^2}-\varepsilon_1(\omega)}{2}} \qquad (4)$$

Reflectivity:

$$R(\omega) = \frac{(n(\omega)-1)^2+k(\omega)^2}{(n(\omega)+1)^2+k(\omega)^2} \qquad (5)$$

Optical conductivity:

$$\sigma(\omega) = \frac{\omega}{4\pi}\varepsilon_2(\omega) \qquad (6)$$

where: ω is frequency, c is speed of light $(3 \times 10^8 ms^{-1})$, $\varepsilon_1(\omega)$ is real part of complex dielectric function and $\varepsilon_2(\omega)$ imaginary part of complex dielectric function.

4. RESULTS

4.1 Optimization of Parameters

The self-consistency cycle accuracy parameters were also kept constant for each material. The optimized strings for Spin, Relativistic and Mixer obtained in previous simulation were also adopted here. The other optimized parameters obtained for each of materials are given in Table 3. These values of optimized parameters are used in subsequent simulations.

Table 3 *Optimized value of Parameters*

Material	**Parameters (Tag)**			
	Occupation type: Gaussian	n_max_pulay	charge_mix_ param	initial moment
$CH_3NH_3GeBr_3$	0.01	5.0	0.8	2.0
$CH_3NH_3GeI_3$	0.01	5.0	0.8	2.0
$CH_3NH_3PbI_3$	0.01	5.0	0.2	2.0
$CH_3NH_3SiI_3$	0.01	10	0.5	2.0
$CH_3NH_3SnI_3$	0.01	7.0	0.2	2.0

4.2 Lattice Constant

The lattice constants determined for each of the materials is given in Table 4 along with some reported theoretical and experimental values where available. The lattice constants are given in the Angstrom (Å) unit.

Table 4 *Lattice Constant in Angstrom (Å)*

Material	**This work**			**Reported**	
	From Series of Single point calculations	From phonopy without ZPE	From phonopy with ZPE	Theoretical	Experimental
$CH_3NH_3GeBr_3$	5.833	5.877	5.894	-	-
$CH_3NH_3GeI_3$	5.933	5.876	5.907	5.907[27]	6.183 [28]
$CH_3NH_3PbI_3$	6.333	6.177	6.248	6.217(Yuan *et a*l., 2015)	6.28(Yuan *et al.*, 2015)
$CH_3NH_3SiI_3$	5.933	5.951	5.950	-	-
$CH_3NH_3SnI_3$	6.033	6.026	6.049	6.163(Yuan *et a*l., 2015)	6.24[29]

The lattice constants obtained using phonopy with ZPE gave values that have a difference of $-0.51, -4.46$ and -3.01% for $CH_3NH_3PbI_3$, $CH_3NH_3GeI_3$ and $CH_3NH_3SnI_3$ respectively with experimental reported values. The lattice constant obtained using phonopy with ZPE (with blyp functional) for $CH_3NH_3GeI_3$ is same with value (5.907 Å) obtained by Umadevi and Watson (2019) using a hybrid functional (PBEsol+D3). There is a difference of $+0.5\%$ for $CH_3NH_3PbI_3$ and a difference of -1.85% for $CH_3NH_3SnI_3$ with values obtained by Yuan *et al,* (2015) using the Heyd–Scuseria–Ernzerhof (HSE) exchange-correlation functional. Thus, the lattice constants obtained for the other materials using phonopy with ZPE can be, with good reason, be taken as a good approximation of their respective lattice constants. With the exception of $CH_3NH_3GeBr_3$ and

$CH_3NH_3SiI_3$ the calculations using phonopy with zero-point energy yield results (i.e. 5.907, 6.248 and 6.049 for $CH_3NH_3GeI_3$, $CH_3NH_3PbI_3$ and $CH_3NH_3SnI_3$ respectively) that have better agreement with experimental values.

4.3 Bandgap Analysis

The LUMO, HOMO and energy band gap calculated in this work are listed in Table 5 along with reported theoretical and experimental band gap values.

Table 5 *LUMO, HOMO and Energy Band Gap*

Material	**LUMO (eV)**	**HOMO (eV)**	**Band Gap (eV)**		
			This work	Reported	
				Theoretical	Experimental
$CH_3NH_3GeBr_3$	-3.85925193	-5.78400997	1.925	-	-
$CH_3NH_3GeI_3$	-3.60616747	-5.21226324	1.606	1.54[30] 2.0[31] 1.60(Umadevi and Watson, 2019)	1.90 (Stoumpos *et al.*, 2015)
$CH_3NH_3PbI_3$	-3.79069858	-5.30338470	1.513	1.662[12] 1.48 [32]	1.61[33]
$CH_3NH_3SiI_3$	-4.05936823	-5.86287715	1.804	-	-
$CH_3NH_3SnI_3$	-4.07492815	-5.12601223	1.051	0.169[12]	1.30[34]

The LUMO level for $CH_3NH_3GeI_3$ is above the CBE of most anode materials, this indicate that it can serve as good solar cell light harvesters. $CH_3NH_3SiI_3$ and $CH_3NH_3GeBr_3$ show good promise as their LUMO level is just below the conduction band edge (CBE) of most anode materials. The suitability of using $CH_3NH_3PbI_3$and $CH_3NH_3SnI_3$as solar cell's light harvesters was already been established. The bandgap evaluated in this work for $CH_3NH_3PbI_3$ and $CH_3NH_3SnI_3$ have a difference of about -6.01% and -1.92% respectively with experimental reported values while for $CH_3NH_3GeI_3$ there is a difference of -15.4 % compare with reported experimental value, but with a much small deviation with reported theoretical values (Table 5). The crystal momentum of electrons and holes are the same in both the LUMO and the HOMO for all the organometallic perovskites i.e., $CH_3NH_3GeI_3$, $CH_3NH_3SiI_3$, $CH_3NH_3GeBr_3$ $CH_3NH_3PbI_3$ and $CH_3NH_3SnI_3$ as such their fundamental band gaps are direct in nature. An energy band gap of 1.606, 1.513, 1.804, 1.051 and 1.925 eV were obtained for CH3NH3GeI3, CH3NH3PbI3, CH3NH3SiI3, CH3NH3SnI3 and CH3NH3GeBr3 respectively. Direct-bandgap materials emit light efficiently because electrons can drop directly from

the conduction band (LUMO) to the valence band (HOMO) without changing their momentum, which requires interactions that can drain away energy [35].

4.4 Real components of Linear Dielectric Function

The graph of real components of linear dielectric function against frequency for cubic directions [100], [010], [001] and [111] are shown in Figures 2 (a) to 2(e).

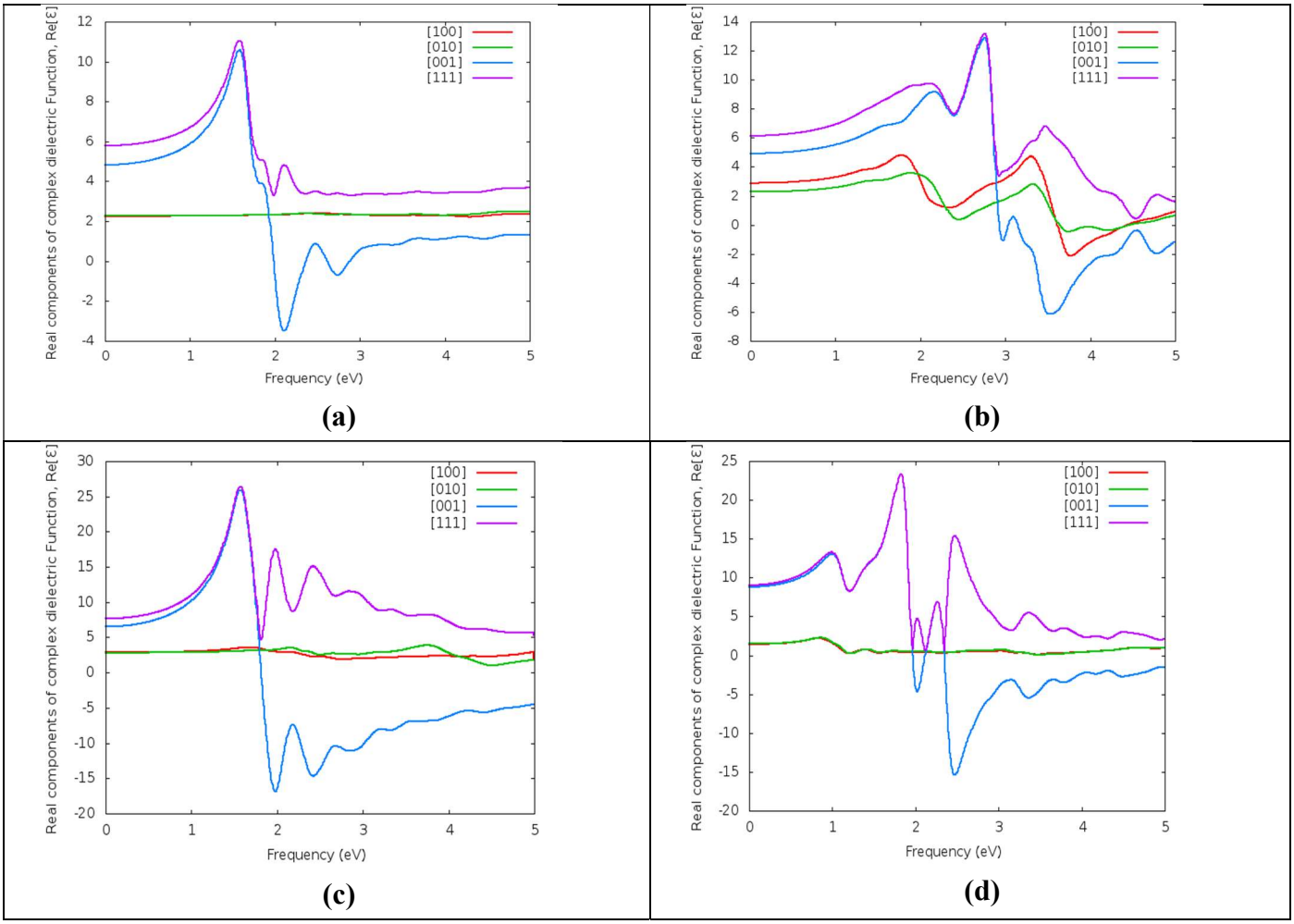

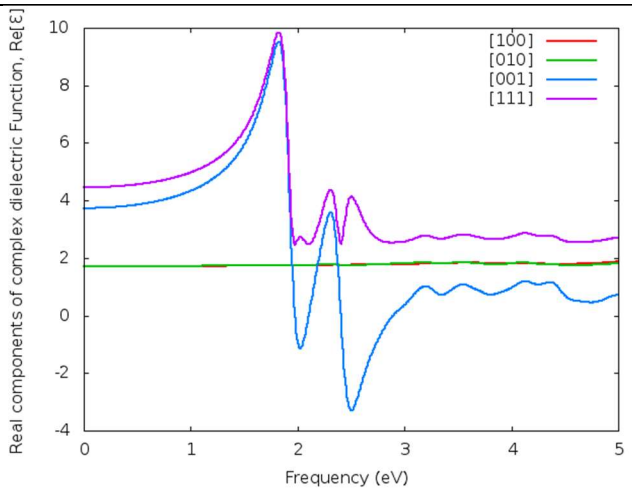

(e)

Figure 2 *Graph of Real Components of Complex Dielectric Tensor against Frequency for* ***(a)*** *$CH_3NH_3GeI_3$* ***(b)*** *$CH_3NH_3PbI_3$* ***(c)*** *$CH_3NH_3SiI_3$* ***(d)*** *$CH_3NH_3SnI_3$,* ***(e)*** *$CH_3NH_3GeBr_3$*

The dielectric constant (relative permittivity) which is value of the real part of the linear dielectric constant at frequency equals to zero (i.e. $Re[\epsilon_r(\omega = 0)]$), are given in Table 6 for each of the above directions.

Table 6: Dielectric Constant (ϵ)

Material	$\boldsymbol{Re[\epsilon_r(\omega = 0)]}$				
	This work				Reported
	[100]	[010]	[001]	[111]	[111]
$CH_3NH_3GeI_3$	2.26	2.27	4.83	5.79	-
$CH_3NH_3PbI_3$	2.88	2.28	4.92	6.14	6.5[36]
$CH_3NH_3SiI_3$	2.86	2.84	6.52	7.67	-
$CH_3NH_3SnI_3$	1.44	1.48	8.8	9.04	8.2[37]
$CH_3NH_3GeBr_3$	1.72	1.72	3.73	4.46	-

In Table 6, it is observed that for all the materials, the dielectric constant (relative permittivity) at the [100] and [010] directions have very close values implying that their electric properties are similar along these directions. Dielectric constants obtained at [001] directions are higher than the ones at [100] and [010] directions. While the relative permittivity at the [111] directions have the highest values for of all the materials. The differences in the dielectric constants obtained in these directions imply that the dielectric property of these materials is anisotropy. The dielectric constants obtain at the [111] directions are close to the reported values; with an underestimation of 5.54% for

$CH_3NH_3PbI_3$ and overestimation of 10.2% for $CH_3NH_3SnI_3$. But the dielectric constants obtain at the [001] direction for $CH_3NH_3SnI_3$is much closer to reported values with an overestimation of 7.34%.

4.5 Optical Properties

The following optical properties; optical absorption coefficient $\alpha(\omega)$, refractive index $n(\omega)$, extinction coefficient $k(\omega)$, reflectivity $R(\omega)$ and optical conductivity $\sigma(\omega)$, were obtained from the frequency dependent complex dielectric function using equations 2 to 6. In a study by Sa *et al*, (2020) on lead-free perovskites ($MABa_{x-1}$ Sn_xI_3 and $MABa_{x-1}$ Si_xI_3), the optical absorption coefficients of the proposed lead-free perovskites are stronger than that of $MAPbI_3$ in the range of 500-800 nm[38].

Optical Absorption Coefficient

The optical absorption coefficient of a material gives information about the optimal solar energy conversion efficiency which is important for the practical application of a material in solar cell. The calculated optical absorption spectra of the considered compounds are presented in Figure 3, In general, there are mainly three light absorption peaks observed for all compounds. The considered compounds show high absorption between the energy ranges from 1.5 to 4.5 eV, with highest peaks at about 2.5 eV for $CH_3NH_3GeBr_3$, $CH_3NH_3SiI_3$ and $CH_3NH_3SnI_3$, while $CH_3NH_3PbI_3$ and $CH_3NH_3GeI_3$ have highest peaks at about 3.5 and 2 eV respectively. The replacement of Pb by Sn, Si or Ge affects the magnitude of the absorption spectra, but the position of the first group of peaks remains at the same frequency. However, the replacement of I by Br in $CH_3NH_3GeI_3$ shift the position of the peaks towards the higher frequency. $CH_3NH_3SiI_3$ and $CH_3NH_3SnI_3$ have maximum absorption second to $CH_3NH_3PbI_3$. Therefore, Sn and Si would be a better substitute of Pb in the organometallic perovskites for application that requires high absorption rate.

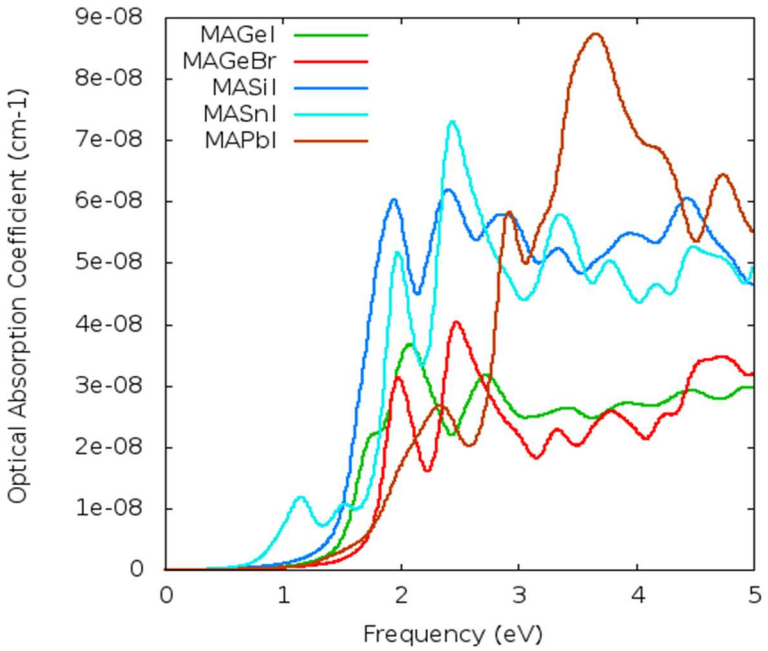

Figure 3 *Graph of Optical Absorption Coefficient against Frequency*

Refractive Index

The knowledge of refractive index is important for the applications of a material in optical devices like solar cell, photo-detector, waveguide and photonic crystal[39]. The overall features of the refractive index for the considered perovskites are qualitatively same in the entire frequency range except some variation in heights and positions of peaks (Figure 4). However, the value of the static refractive index $n(\omega = 0)$ is different for each material, the maximum value of $n(\omega = 0)$ is found as 3.42 for $CH_3NH_3SnI_3$ while the minimum value if found for $CH_3NH_3GeBr_3$ as 1.64.

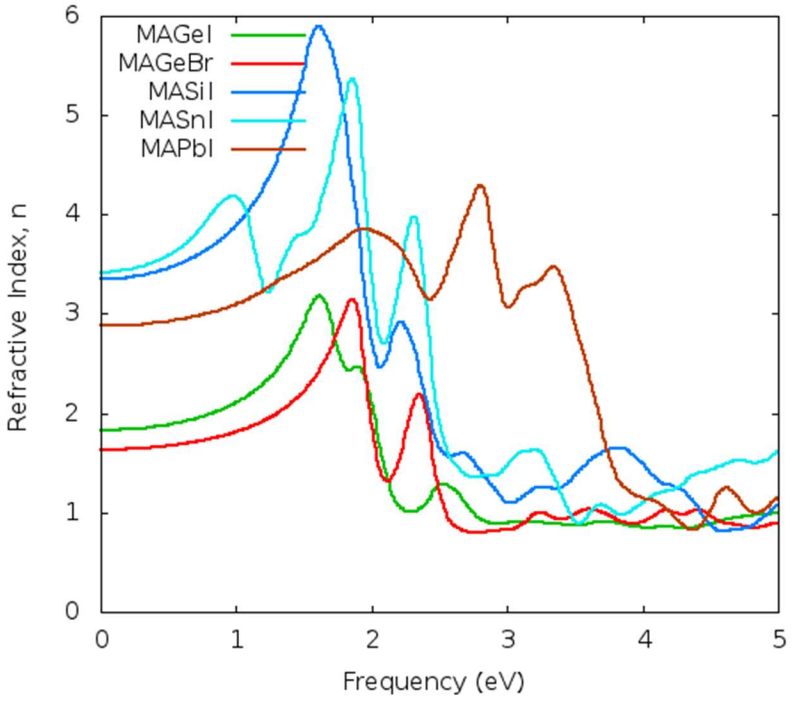

Figure 4 *Graph of Refractive Index against Frequency*

Extinction index

From figure 5, $CH_3NH_3SnI_3$ has the highest attenuation rate while $CH_3NH_3GeI_3$ has the lowest. The peaks are concentrated around the frequency range of 1.0 to 3.5 eV, which correspond to bandgap range of the materials. High values of **k** at frequency range of 1.0 to 3.5 eV (wavelength of 1241 to 354 nm) shows that these materials have higher opacity at this range.

Reflectivity

Reflectivity is another important optical property for the solar cell and other applications of the perovskite. All the investigated perovskite materials show a low reflectivity (see Figure 6) in the range of about 0.131 to 0.261. This low reflectivity suggests that the materials have high absorptivity[40], as such they will function well as light harvester.

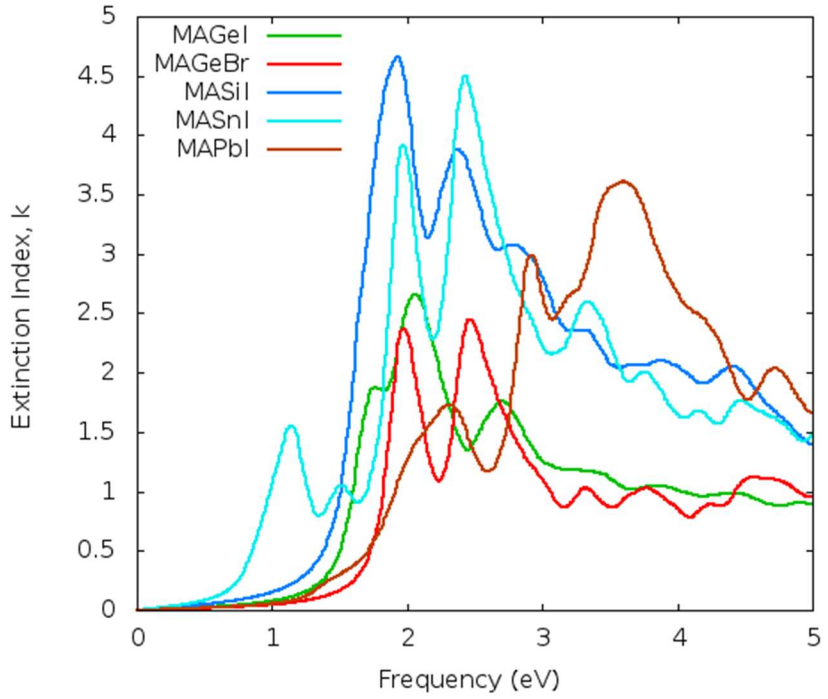

Figure 5 *Graph of Extinction index against Frequency*

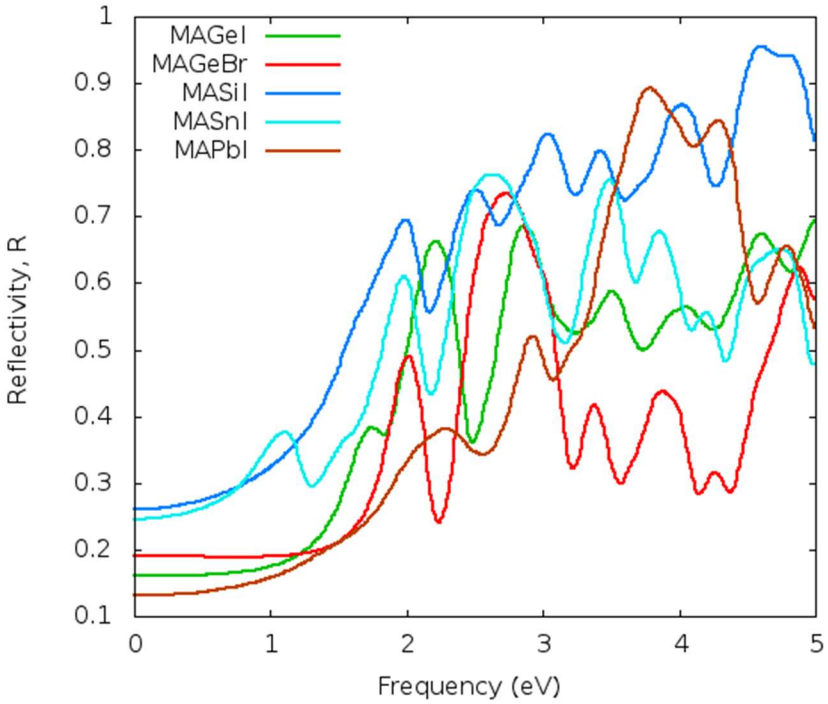

Figure 6 *Graph of Reflectivity against Frequency*

Optical Conductivity

Figure 7 shows the optical conductivity spectra of the materials. The optical conductivity spectrum of $CH_3NH_3SnI_3$ is highest with maxima of the peak at about 1.7 eV, while the conductivity spectrum of $CH_3NH_3GeI_3$ is lowest with maxima at 1.9 eV. The major peaks are located within the frequency range of $\omega = 1.5$ to 3 eV for all the materials, similar to the phenomenon observed in extinction index.

.

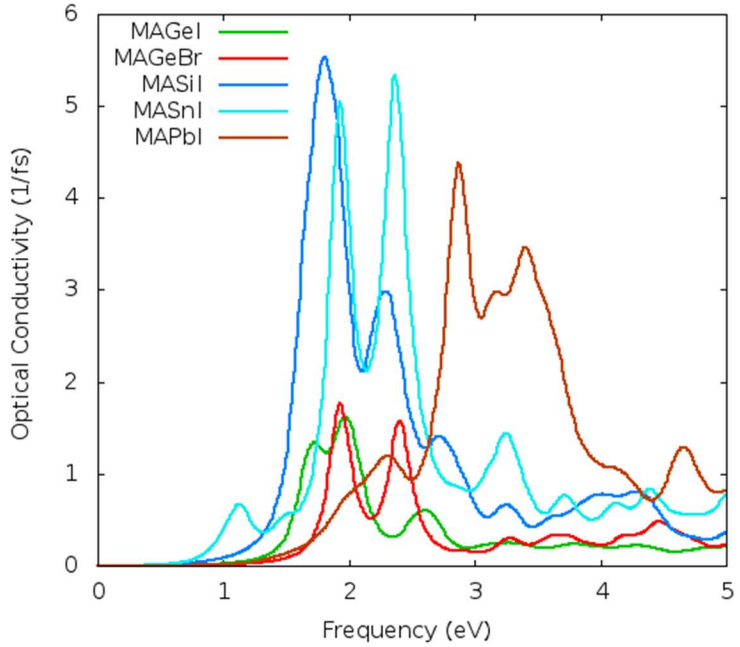

Figure 7 *Graph of Optical Conductivity against Frequency*

4.6 Summary of results

The summary of calculated properties (physical, electronic and optical) of the lead-free materials presented in Table 7. Depending on the choice of area of application, these materials can be used in different areas of optoelectronic applications.

***Table** 7. Sunnary of Results*

S/N	Properties	Decreasing Order ≫				
1.	Lattice constant(Å)	$CH_3NH_3PbI_3$	$CH_3NH_3SnI_3$	$CH_3NH_3SiI_3$	$CH_3NH_3GeI_3$	$CH_3NH_3GeBr_3$
		6.248	**6.049**	**5.950**	**5.933**	**5.833**
2.	Bandgap(eV)	$CH_3NH_3GeBr_3$	$CH_3NH_3SiI_3$	$CH_3NH_3GeI_3$	$CH_3NH_3PbI_3$	$CH_3NH_3SnI_3$
		1.925	**1.804**	**1.606**	**1.513**	**1.051**
3.	Dielectric Constant [111]	$CH_3NH_3SnI_3$	$CH_3NH_3SiI_3$	$CH_3NH_3PbI_3$	$CH_3NH_3GeI_3$	$CH_3NH_3GeBr_3$
		9.04	**7.67**	**6.14**	**5.79**	**4.46**
4.	Static Refractive index	$CH_3NH_3SnI_3$	$CH_3NH_3SiI_3$	$CH_3NH_3PbI_3$	$CH_3NH_3GeI_3$	$CH_3NH_3GeBr_3$
		3.42	**3.35**	**2.88**	**1.83**	**1.64**
5.	Static Reflectivity	$CH_3NH_3SiI_3$	$CH_3NH_3SnI_3$	$CH_3NH_3GeBr_3$	$CH_3NH_3GeI_3$	$CH_3NH_3PbI_3$
		0.261	**0.246**	**0.190**	**0.161**	**0.131**
6.	Optical Absorption spectrum (Highest Peak) (cm^{-1})	$CH_3NH_3PbI_3$	$CH_3NH_3SnI_3$	$CH_3NH_3SiI_3$	$CH_3NH_3GeBr_3$	$CH_3NH_3GeI_3$
		$\mathbf{8.8 \times 10^{-8}}$	$\mathbf{7.2 \times 10^{-8}}$	$\mathbf{6.2 \times 10^{-8}}$	$\mathbf{4.0 \times 10^{-8}}$	$\mathbf{3.5 \times 10^{-8}}$
7.	Optical Conductivity spectrum (Highest Peak) $(1/fs)$	$CH_3NH_3SnI_3$	$CH_3NH_3SiI_3$	$CH_3NH_3PbI_3$	$CH_3NH_3GeBr_3$	$CH_3NH_3GeI_3$
		5.5	**5.25**	**4.25**	**1.7**	**1.5**
8.	Extinction Index spectrum (Highest Peak)	$CH_3NH_3SiI_3$	$CH_3NH_3SnI_3$	$CH_3NH_3PbI_3$	$CH_3NH_3GeI_3$	$CH_3NH_3GeBr_3$
		4.7	**3.7**	**3.4**	**2.5**	**2.3**

5. CONCLUSION

In conclusion, the lattice constants of various materials were determined using single point calculations and phonopy with zero-point energy correction. The values obtained using phonopy with ZPE were found to be in good agreement with reported experimental and theoretical values for most materials. Bandgap analysis was also carried out and the LUMO and HOMO levels as well as the energy band gap were determined. The results showed that some materials, such as $CH_3NH_3GeI_3$ and CH3NH3SiI3, have potential as solar cell light harvesters. the dielectric constant (relative permittivity) of the materials studied exhibit anisotropic behavior, with the dielectric constants along the [111] direction having the highest values. The optical absorption coefficients of the materials were found to be high between the energy range of 1.5 to 4.5 eV, with maximum absorption peaks observed at about 2.5 eV for $CH_3NH_3GeBr_3$, $CH_3NH_3SiI_3$ and $CH_3NH_3SnI_3$, while $CH_3NH_3PbI_3$ and

$CH_3NH_3GeI_3$ have maximum peaks at about 3.5 and 2 eV respectively. The refractive index, extinction coefficient, and reflectivity of the materials were also investigated. The results suggest that Sn and Si are better substitutes for Pb in organometallic perovskites for applications that require high absorption rates. Overall, the optical properties studied are important for practical applications in solar cells, photodetectors, waveguides, and photonic crystals.

REFERENCES

1. Arbuznikov, A., *Hybrid exchange correlation functionals and potentials: Concept elaboration.* Journal of Structural Chemistry, 2007. **48**: p. S1-S31.
2. Babayigit, A., et al., *Toxicity of organometal halide perovskite solar cells.* Nature materials, 2016. **15**(3): p. 247-251.
3. Babayigit, A., et al., *Assessing the toxicity of Pb-and Sn-based perovskite solar cells in model organism Danio rerio.* Scientific reports, 2016. **6**(1): p. 1-11.
4. Abate, A., *Perovskite Solar Cells Go Lead Free.* Joule, 2017.
5. Galadanci and G. Babaji, *Computations of the Ground State Cohesive Properties Of AlAs Crystalline Structure Using Fhi-Aims Code.* Journal of Applied Physics, 2013. **4**(5): p. 85-95.
6. Chen, L.-Q. and Y. Gu, *Computational Metallurgy*, in *Physical Metallurgy*. 2014, Elsevier. p. 2807-2835.
7. Owolabi, J., et al., *Determination of Band Structure of Gallium-Arsenide and Aluminium-Arsenide Using Density Functional Theory.* Computational Chemistry, 2016. **4**(03): p. 73-83.
8. Henrich, V.E. and P.A. Cox, *The surface science of metal oxides*. 1996: Cambridge university press.
9. Jiao, Y., F. Zhang, and S. Meng, *Dye sensitized solar cells Principles and new design*, in *Solar Cells-Dye-Sensitized Devices*. 2011, InTech.
10. Kavan, L., et al., *Electrochemical and Photoelectrochemical Investigation of Single-Crystal Anatase.* Journal of American Chemical Society, 1996. **8**(26): p. 6716-6723.
11. Brivio, F., A.B. Walker, and A. Walsh, *Structural and electronic properties of hybrid perovskites for high-efficiency thin-film photovoltaics from first-principles.* Apl Materials, 2013. **1**(4): p. 042111.
12. Yuan, Y., et al., *Nature of the band gap of halide perovskites ABX_3(A= CH_3NH_3,Cs; B = Sn, Pb; X= Cl, Br, I): First-principles calculations.* Chin. Phys. B 2015. **24**(11): p. 5.
13. Yamada, Y., et al., *Photoelectronic Responses in Solution-Processed Perovskite $CH_3NH_3PbI_3$ Solar Cells Studied by Photoluminescence and Photoabsorption Spectroscopy.* IEEE Journal of Photovoltaics, 2015. **5**(1): p. 401-405.
14. Chen, L.-F., et al., *Microwave electronics: measurement and materials characterization*. 2004: John Wiley & Sons.

15. Pedesseau, L., et al. *Dielectric properties of hybrid perovskites and drift-diffusion modeling of perovskite cells*. in *Physics, Simulation, and Photonic Engineering of Photovoltaic Devices V*. 2016. International Society for Optics and Photonics.
16. QuantumWise. *Optical Properties of Silicon*. Reference Manual 2017 [cited 2017 23 November]; Available from: https://docs.quantumwise.com/v2017/tutorials/optical/optical.html#optical-spectrum.
17. Park, N.-G., *Methodologies for high efficiency perovskite solar cells.* Nano convergence, 2016. **3**(1): p. 1-13.
18. Dresselhaus, M., *Solid State Physics (Part II): Optical Properties of Solids* Retrieved from Lecture Notes Online Web site: http://bookos.org/book/453978/572abc, 2001. **190**.
19. Saha, S., T. Sinha, and A. Mookerjee, *Electronic structure, chemical bonding, and optical properties of paraelectric BaTiO 3.* Physical Review B, 2000. **62**(13): p. 8828.
20. Wang, L., *Measuring optical absorption coefficient of pure water in UV using the integrating cavity absorption meter*. 2008, Texas A&M University.
21. Gervais, F., *Optical conductivity of oxides.* Materials Science and Engineering: R: Reports, 2002. **39**(2-3): p. 29-92.
22. Valizade, M., M. Heyhat, and M. Maerefat, *Experimental comparison of optical properties of nanofluid and metal foam for using in direct absorption solar collectors.* Solar Energy Materials and Solar Cells, 2019. **195**: p. 71-80.
23. Ujihara, K., *Reflectivity of metals at high temperatures.* Journal of Applied Physics, 1972. **43**(5): p. 2376-2383.
24. Afromowitz, M.A., *Refractive index of Ga1− xAlxAs.* Solid State Communications, 1974. **15**(1): p. 59-63.
25. Oku, T., *Crystal structures of $CH_3NH_3PbI_3$ and related perovskite compounds used for solar cells*, in *Solar Cells-New Approaches and Reviews*. 2015, InTech.
26. Chen, C., et al., *Nonlinear optical borate crystals: Principals and applications*. 2012: John Wiley & Sons.
27. Umadevi, D. and G.W. Watson, *Quasiparticle GW Calculations on Lead-Free Hybrid Germanium Iodide Perovskite CH3NH3GeI3 for Photovoltaic Applications.* ACS Omega, 2019. **4**(3): p. 5661-5669.
28. Stoumpos, C.C. and M.G. Kanatzidis, *The renaissance of halide perovskites and their evolution as emerging semiconductors.* Accounts of chemical research, 2015. **48**(10): p. 2791-2802.
29. Yamada, K., et al., *Structural Phase Transition and Electrical Conductivity of the Perovskite CH3NH3Sn1-x Pb x Br3 and CsSnBr3.* Bulletin of the Chemical Society of Japan, 1990. **63**(9): p. 2521-2525.

30. Yuqiu, J., et al., *Exploring electronic and optical properties of $CH_3NH_3GeI_3$ perovskite: Insights from the first principles.* Computational and Theoretical Chemistry, 2017. **1114**: p. 20-24.
31. Hoefler, S.F., G. Trimmel, and T. Rath, *Progress on lead-free metal halide perovskites for photovoltaic applications: a review.* Monatsh Chem, 2017. **148**(5): p. 795-826.
32. Ahmed, T., et al., *Optical properties of organometallic perovskite: An ab initio study using relativistic GW correction and Bethe-Salpeter equation.* EPL (Europhysics Letters), 2015. **108**(6): p. 67015.
33. Heyd, J., G.E. Scuseria, and M. Ernzerhof, *Hybrid functionals based on a screened Coulomb potential.* The Journal of Chemical Physics, 2006. **118**(18): p. 8207-8215.
34. Xu, B., et al., *Carbazole-Based Hole-Transport Materials for Efficient Solid-State Dye-Sensitized Solar Cells and Perovskite Solar Cells.* Advanced Materials, 2014. **26**(38): p. 6629-6634.
35. Hecht, J., *Indirect and Direct Band Gaps*, in *Understanding lasers: an entry-level guide*. 2018, John Wiley & Sons.
36. Hirasawa, M., et al., *Magnetoabsorption of the lowest exciton in perovskite-type compound $(CH_3NH_3)PbI_3$.* Physica B 1994. **201**: p. 427-430.
37. Umari, P., E. Mosconi, and F. De Angelis, *Relativistic GW calculations on $CH_3NH_3PbI_3$ and $CH_3NH_3SnI_3$ perovskites for solar cell applications.* Scientific reports, 2014. **4**: p. 4467.
38. Sa, R., et al., *Stable lead-free perovskite solar cells: A first-principles investigation.* Spectrochimica Acta Part A: Molecular and Biomolecular Spectroscopy, 2020. **239**: p. 118493.
39. Hoffman, J.B., A.L. Schleper, and P.V. Kamat, *Transformation of sintered $CsPbBr_3$ nanocrystals to cubic $CsPbI_3$ and gradient $CsPbBr_x I_{3-x}$ through halide exchange.* Journal of the American Chemical Society, 2016. **138**(27): p. 8603-8611.
40. Roknuzzaman, M., et al., *Towards lead-free perovskite photovoltaics and optoelectronics by ab-initio simulations.* Scientific reports, 2017. **7**(1): p. 14025.